REPORTS

NONLINEAR OPTICS

Large optical nonlinearity of indium tin oxide in its epsilon-near-zero region

M. Zahirul Alam,[1] Israel De Leon,[1,3]* Robert W. Boyd[1,2]

Nonlinear optical phenomena are crucial for a broad range of applications, such as microscopy, all-optical data processing, and quantum information. However, materials usually exhibit a weak optical nonlinearity even under intense coherent illumination. We report that indium tin oxide can acquire an ultrafast and large intensity-dependent refractive index in the region of the spectrum where the real part of its permittivity vanishes. We observe a change in the real part of the refractive index of 0.72 ± 0.025, corresponding to 170% of the linear refractive index. This change in refractive index is reversible with a recovery time of about 360 femtoseconds. Our results offer the possibility of designing material structures with large ultrafast nonlinearity for applications in nanophotonics.

A long-standing goal in nonlinear optics has been the development of materials whose refractive index can be drastically changed using a low-power optical field. Ideally, these materials should possess sub-picosecond time response and be compatible with existing complementary metal-oxide semiconductor (CMOS) fabrication technologies (*1*–*2*). Simple calculus shows that, for a given change ($\Delta\varepsilon$) in the permittivity ε, the resulting change (Δn) in the refractive index n is given for a lossless material by $\Delta n = \Delta\varepsilon/(2\sqrt{\varepsilon})$. We see that this change becomes large as the permittivity becomes small, suggesting that the epsilon-near-zero (ENZ) frequencies of a material system should give rise to strong nonlinear optical properties.

Materials possessing free charges, such as metals and highly doped semiconductors, have zero real permittivity at the bulk plasmon wavelength. A number of authors have reported on the unusual properties of matter under ENZ conditions (*3*–*5*) and on their promise for applications in nonlinear optics (*6*–*10*).

We used commercially available indium tin oxide (ITO), a CMOS-compatible degenerate semiconductor, as the ENZ medium (Fig. 1). The zero-permittivity wavelength of ITO occurs at near-infrared wavelengths and can be tuned by controlling the doping density or by applying a static electric field (*11*, *12*). The *z*-scan technique was used to characterize the intensity-dependent refractive index of ITO for transverse magnetic (TM) polarized light (Fig. 2A) (*13*, *14*). The wavelength-dependent effective nonlinear refractive index coefficient $n_{2(\mathrm{eff})} = \Delta n/I$ (I is the intensity of the laser beam) and effective nonlinear attenuation constant $\beta_{(\mathrm{eff})} = \Delta\alpha/I$ extracted from our measurements are plotted for angles of incidence varying from θ = 0° to θ = 60° (Fig. 2, A and B). The results indicate that ITO exhibits positive $n_{2(\mathrm{eff})}$ and negative $\beta_{(\mathrm{eff})}$, corresponding to self-focusing and saturable absorption, respectively. Our results reveal a substantial wavelength- and angle-dependent enhancement of the material's nonlinear response at ENZ wavelengths. The measured value of $n_{2(\mathrm{eff})}$ (6×10^{-5} cm^2/GW) at the shortest wavelength (970 nm) agrees well with the value reported by Elim *et al.* (*15*). At a wavelength of 1240 nm for normal incidence, $n_{2(\mathrm{eff})}$ and $\beta_{(\mathrm{eff})}$ are ~43 and ~53 times larger than the corresponding values at 970 nm, respectively. For TM-polarized light at oblique incident, the nonlinear response is further enhanced. The enhancement factors, defined relative to the values far from the ENZ spectral region (at λ = 970 nm) at normal incidence, are plotted as functions of θ in Fig. 2C. The enhancement tends to increase with θ for 0° < θ < 60° and decreases sharply for θ > 60°. The maximum enhancement factors, measured at θ = 60°, are 1837 and 2377 for $n_{2(\mathrm{eff})}$ and $\beta_{(\mathrm{eff})}$, respectively. Thus, at λ_0 = 1240 nm, the $n_{2(\mathrm{eff})}$ and $\beta_{(\mathrm{eff})}$ values for θ = 60° are ~43 and ~45 times larger than for normal incidence, respectively.

The temporal dynamics of the optical nonlinear response was studied using a degenerate pump-probe transmission measurement. Here, an intense pump pulse and a weak probe pulse at the same wavelength interact with the sample, and the induced change in probe transmittance ΔT is measured as a function to the time delay τ between the two pulses. The measured temporal response is proportional to the convolution of the probe's temporal envelope with the material's temporal response function. (Fig. 2D). The transient nonlinear response has a rise time no longer than 200 fs (this estimate is limited by our laser pulse duration) and a recovery time of 360 fs. Such ultrafast response would allow all-optical modulation speeds of at least 1.5 THz.

The nonlinear coefficients shown in Fig. 2, A and B, may be slightly overestimated because the *z*-scan method neglects the change in reflectivity caused by Δn (*16*), but this overestimation is no larger than by a factor of ~1.8. In any case, the measured values are extremely large. In particular, the value of $n_{2(\mathrm{eff})}$ = 0.11 cm^2/GW measured at θ = 60° is more than two orders of magnitude larger than that of As_2Se_3 chalcogenide glass (*17*) and ~5 times larger in magnitude than that of a recently proposed highly nonlinear metamaterial (*6*). The optical losses of ITO at ENZ wavelengths can be quite large, although in (*16*) we describe some realistic applications that can tolerate this much loss.

We attribute the observed nonlinearity primarily to a modification of the energy distribution of conduction-band electrons as a consequence of the laser-induced electron heating. We describe the nonlinear optical response by means of a phenomenological two-temperature model (*16*, *18*–*20*). Figure 3A shows the calculated temporal evolution of the free-electron temperature (T_e) and lattice temperature (T_l) of ITO after irradiation by the laser pulse (denoted by the dashed curve). The free-electron temperature exhibits an ultrafast transient and is limited by the electron-phonon relaxation time of the material (*21*). The normalized transient nonlinear response measured via the degenerate pump-probe technique is well described by the temporal profiles of T_e convolved with the probe's intensity envelope, which is plotted as the solid curve in Fig. 2D.

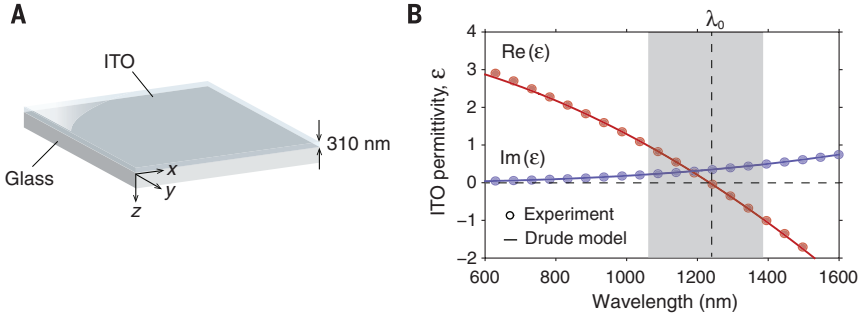

Fig. 1. The ITO sample under investigation and its linear optical response. (**A**) Structure under investigation. (**B**) Linear relative permittivity of the ITO film measured via spectroscopic ellipsometry (symbols) and estimated by the Drude model (lines). The condition Re(ε) = 0 occurs at λ_0 = 1240 nm. The shaded region shows the spectral range investigated in our nonlinear optical characterization.

[1]Department of Physics and Max Planck Centre for Extreme and Quantum Photonics, University of Ottawa, 25 Templeton Street, Ottawa, ON, K1N 6N5, Canada. [2]Institute of Optics and Department of Physics and Astronomy, University of Rochester, Rochester, NY 14627, USA. [3]School of Engineering and Sciences, Tecnológico de Monterrey, Monterrey, Nuevo León 64849, Mexico.
*Corresponding author. Email: ideleon@itesm.mx

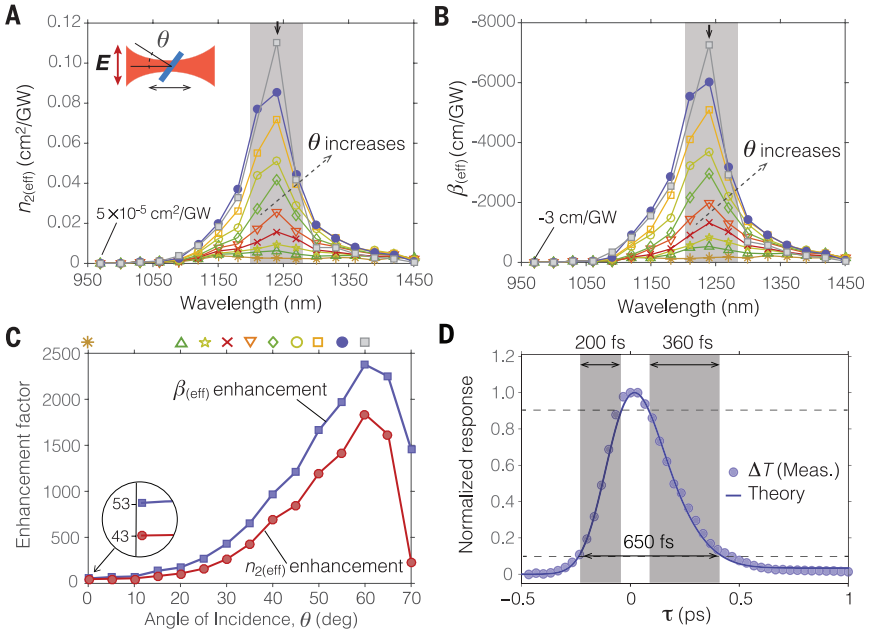

Fig. 2. Nonlinear optical response of the ITO sample. Wavelength dependence of (**A**) the nonlinear effective refractive index, $n_{2(eff)}$, and (**B**) the effective nonlinear attenuation constant, $\beta_{(eff)}$. The nonlinear response is enhanced in the ENZ region of the spectrum (shaded). The vertical arrows indicate the wavelength λ_0 = 1240 nm. (**C**) The corresponding enhancement for $n_{2(eff)}$ and $\beta_{(eff)}$ at λ_0, compared with values at 970 nm, are plotted as functions of θ. The values of θ corresponding to the different symbols in (A) and (B) are indicated at the top. (**D**) Time dependence of the normalized transient change of transmittance (ΔT) obtained via a degenerate pump-probe measurement.

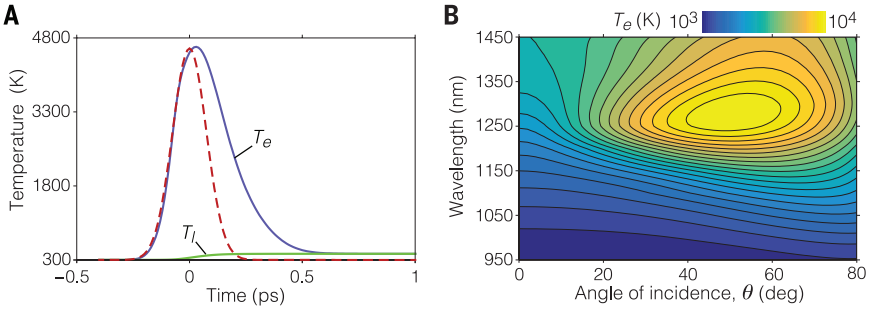

Fig. 3. Numerical modeling of the hot-electron dynamics of ITO. (**A**) Transient response of T_e and T_l obtained using the two-temperature model. The dashed curve denotes the pulse intensity profile (in arbitrary units). (**B**) Map of the peak free-electron temperature in ITO calculated as a function of θ and λ. Both calculations assume a normally incident laser with an intensity of 66 GW/cm^2.

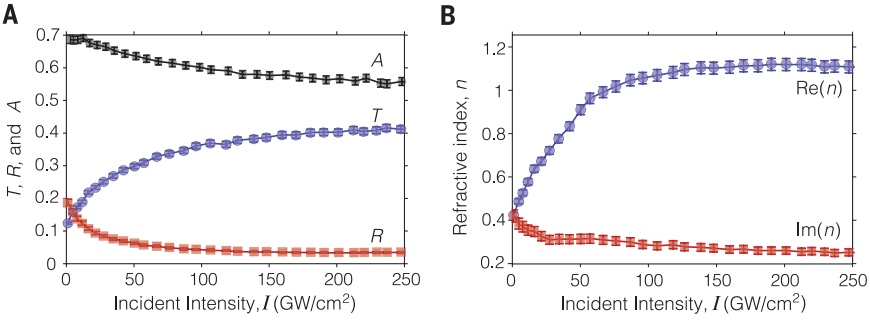

Fig. 4. Nonlinear optical response of ITO for laser fields sufficiently intense to produce saturation. (**A**) Intensity-dependent transmittance (T), reflectance (R), and absorptance (A) of the ITO-glass structure at λ_0 for θ = 30°. (**B**) Complex effective refractive index of ITO extracted from the measured values in (A) using a transfer-matrix method.

The peak values of T_e obtained with our model are plotted in Fig. 3B as functions of the wavelength and the angle of incidence. The temperature profile exhibits the main features present in our experimental results, namely a pronounced enhancement of the response at ENZ wavelengths that reaches a maximum for an angle of incidence close to θ = 60°. The general behavior observed in this result can be understood in terms of two contributions. The increasing values of T_e for longer wavelengths result from the increase in free carrier absorption, and the peak that develops around θ ≈ 60° results from an enhancement of the electric field within the ITO film. This enhancement occurs only for obliquely incident TM polarized light at wavelengths within the ENZ region and follows from the continuity of the normal electric displacement field across an ITO-air interface (*16*, *22*). As discussed in (*16*), Δε results from an effective red shift in the material's plasma frequency caused by an increase in the free-electron temperature (ΔT_e). It is important to note that Δε does not scale linearly with ΔT_e for a large ΔT_e and that Δn is a nonlinear function of Δε at ENZ. Consequently, a modest field intensity enhancement in the ITO film can lead to a large enhancement of $n_{2(eff)}$ at ENZ wavelengths. This is confirmed by our model presented in (*16*), which accounts for such nonlinear relationships between Δn, Δε, and ΔT_e.

The hot-electron–induced optical nonlinearity of ITO at ENZ wavelengths differs from that of noble metals under infrared irradiation in two ways. First, as argued above, for a given change in permittivity, the nonlinear change in refractive index is always larger in the ENZ region than in non-ENZ regions. Second, the free-electron heat capacity of ITO (4.53 Jm^{-3}K^{-1}) is more than an order of magnitude smaller than that of a noble metal such as gold. Thus, the increase in the free-electron temperature compared with the Fermi temperature and the consequent change in refractive index in ITO is much larger.

For sufficiently large optical intensities, the nonlinear response of ITO at ENZ wavelengths can lead to changes in its refractive index that are larger than the linear refractive index. As a result, the Fresnel reflection and transmission coefficients undergo a large change as a function of the incident optical intensity. To demonstrate this phenomenon, we measured the intensity-dependent transmittance (T), reflectance (R), and absorptance (A) of the sample at 1240 nm for θ = 30° (Fig. 4A). At the lowest intensity, these measurements agree well with the predictions of a simple linear Fresnel analysis. As the intensity is increased, we observe a large monotonic increase (reduction) in transmittance (reflectance). The maximum reduction in absorptance is ~30%, which is consistent with the saturable absorption observed in our z-scan measurements. The real part of the refractive index of ITO undergoes a dramatic change from its linear value of 0.42 to a value of 1.14 ± 0.025 for an intensity of 150 GW/cm^2 (Fig. 4B). Similarly, the imaginary part of the index is substantially reduced from

its linear value of 0.42 to a value of 0.27 ± 0.015 at this intensity. Both the real and the imaginary parts of the refractive index saturate for even higher input power. We found that these measurements are highly repeatable and that the material does not exhibit a permanent change of its optical properties.

The magnitude of the optically induced ultrafast change of the real part of the refractive index (Δn = 0.72 ± 0.025) and the relative change of 170% in comparison to the linear value are unprecedented. The change in the refractive index corresponds to a change of the permittivity from $\varepsilon = 0 + 0.352i$ to $\varepsilon = 1.22 + 0.61i$ where i is the square root of −1. This result shows that ITO can exhibit a reversible transition from metallic to a lossy dielectric state with a subpicosecond time response at wavelengths slightly longer than the bulk plasmon wavelength. Moreover, the usual perturbation expansion description of nonlinear optical effects is not applicable for this material at high intensities.

We have shown that a thin ITO film exhibits an extremely large ultrafast third-order nonlinearity at ENZ wavelengths. Moreover, it can acquire an optically induced change in the refractive index that is unprecedentedly large. Our results challenge the notion that the nonlinear optical response is only a perturbation to the linear response. Materials with such a large nonlinear response are expected to enable exotic nonlinear dynamics (*22*) and allow all-optical control of metasurface and active plasmonics devices. Thus, our results introduce a completely new paradigm in nonlinear optics and open new avenues for developing optical nanostructures with large nonlinearity for applications in nanophotonics, plasmonics, and nonlinear nano-optics.

REFERENCES AND NOTES

1. M. Kauranen, A. V. Zayats, *Nat. Photonics* **6**, 737–748 (2012).
2. M. Abb, P. Albella, J. Aizpurua, O. L. Muskens, *Nano Lett.* **11**, 2457–2463 (2011).
3. M. Silveirinha, N. Engheta, *Phys. Rev. Lett.* **97**, 157403 (2006).
4. A. Alù, M. Silveirinha, A. Salandrino, N. Engheta, *Phys. Rev. B* **75**, 155410 (2007).
5. A. R. Davoyan, A. M. Mahmoud, N. Engheta, *Opt. Express* **21**, 3279–3286 (2013).
6. A. D. Neira *et al.*, *Nat. Commun.* **6**, 7757 (2015).
7. H. Suchowski *et al.*, *Science* **342**, 1223–1226 (2013).
8. A. Capretti, Y. Wang, N. Engheta, L. Dal Negro, *Opt. Lett.* **40**, 1500–1503 (2015).
9. T. S. Luk *et al.*, *Appl. Phys. Lett.* **106**, 151103 (2015).
10. N. Kinsey *et al.*, *Optica* **2**, 616 (2015).
11. G. V. Naik, V. M. Shalaev, A. Boltasseva, *Adv. Mater.* **25**, 3264–3294 (2013).
12. E. Feigenbaum, K. Diest, H. A. Atwater, *Nano Lett.* **10**, 2111–2116 (2010).
13. M. Sheik-Bahae, A. A. Said, T.-H. Wei, D. J. Hagan, E. W. Van Stryland, *IEEE J. Quantum Electron.* **26**, 760–769 (1990).
14. B. K. Rhee, J. S. Byun, E. W. Van Stryland, *J. Opt. Soc. Am. B* **13**, 2720 (1996).
15. H. I. Elim, W. Ji, F. Zhu, *Appl. Phys. B* **82**, 439–442 (2006).
16. See supplementary materials on *Science* Online.
17. R. W. Boyd, *Nonlinear Optics* (Elsevier, 2008).
18. C. Sun, F. Vallée, L. Acioli, E. P. Ippen, J. G. Fujimoto, *Phys. Rev. B Condens. Matter* **48**, 12365–12368 (1993).
19. S. D. Brorson, J. G. Fujimoto, E. P. Ippen, *Phys. Rev. Lett.* **59**, 1962–1965 (1987).
20. E. Carpene, *Phys. Rev. B* **74**, 024301 (2006).
21. B. Rethfeld, A. Kaiser, M. Vicanek, G. Simon, *Phys. Rev. B* **65**, 214303 (2002).
22. D. de Ceglia, S. Campione, M. A. Vincenti, F. Capolino, M. Scalora, *Phys. Rev. B* **87**, 155140 (2013).

ACKNOWLEDGMENTS

The authors gratefully acknowledge the support of the Canada Excellence Research Chairs Program. R.W.B. is the cofounder and Chief Technology Officer of KBN Optics, Pittsford, NY.

SUPPLEMENTARY MATERIALS

www.sciencemag.org/content/352/6287/795/suppl/DC1
Materials and Methods
Supplementary Text
Figs. S1 to S4
References (*23*–*32*)

7 December 2015; accepted 12 April 2016
Published online 28 April 2016
10.1126/science.aae0330

CATALYSIS

Photochemical route for synthesizing atomically dispersed palladium catalysts

Pengxin Liu,[1] Yun Zhao,[1] Ruixuan Qin,[1] Shiguang Mo,[1] Guangxu Chen,[1] Lin Gu,[2] Daniel M. Chevrier,[3] Peng Zhang,[3] Qing Guo,[1] Dandan Zang,[1] Binghui Wu,[1] Gang Fu,[1]* Nanfeng Zheng[1]*

Atomically dispersed noble metal catalysts often exhibit high catalytic performances, but the metal loading density must be kept low (usually below 0.5%) to avoid the formation of metal nanoparticles through sintering. We report a photochemical strategy to fabricate a stable atomically dispersed palladium–titanium oxide catalyst (Pd_1/TiO_2) on ethylene glycolate (EG)–stabilized ultrathin TiO_2 nanosheets containing Pd up to 1.5%. The Pd_1/TiO_2 catalyst exhibited high catalytic activity in hydrogenation of C=C bonds, exceeding that of surface Pd atoms on commercial Pd catalysts by a factor of 9. No decay in the activity was observed for 20 cycles. More important, the Pd_1/TiO_2-EG system could activate H_2 in a heterolytic pathway, leading to a catalytic enhancement in hydrogenation of aldehydes by a factor of more than 55.

Atomically dispersed catalysts with mononuclear metal complexes or single metal atoms anchored on supports have recently attracted increasing research attention (*1*–*15*). With 100% metal dispersity, atomically dispersed catalysts offer the maximum atom efficiency, providing the most ideal strategy to create cost-effective catalysts, particularly those based on Earth-scarce metals such as Pt (*1*–*5*), Au (*5*–*8*), Pd (*9*–*12*), and Ir (*13*, *14*). Moreover, the uniform active sites of atomically dispersed catalysts make them a model system to understand heterogeneous catalysis at the molecular level (*4*, *6*, *10*, *12*–*14*, *16*–*21*), bridging the gap between heterogeneous and homogeneous catalysis.

During the past decade, several strategies for atomically dispersing metal sites on catalyst supports have emerged; these include lowering the loading amount of metal components (*1*, *8*–*10*, *12*, *20*), enhancing the metal-support interactions (*4*, *6*, *9*, *19*), and using voids in supports or vacancy defects on supports (*3*, *11*, *14*, *22*). In most cases, the supports for atomically dispersed catalysts are deliberately chosen. Zeolites provide effective voids to anchor individual metal atoms therein and prevent them from sintering during catalysis (*23*, *24*). Defects on reducible oxides (e.g., TiO_2 and CeO_2) (*25*, *26*) and on graphene or C_3N_4 (*9*, *11*, *22*) help to stabilize atomically dispersed metal atoms on supports. Coordinatively unsaturated Al^{3+} ions on γ-Al_2O_3 act as binding centers to maintain the high dispersion of Pt atoms, but Pt rafts form as the loading amount of Pt increases (*3*). Currently, two major challenges remain in the field of atomically dispersed catalysts: (i) to ensure a loading content high enough for practical applications while maintaining the metal centers as individual sites under catalytic conditions (*27*, *28*), and (ii) to address whether atomically dispersed catalysts offer distinct active sites and/or undergo catalytic pathways different from those of conventional metal catalysts (*1*, *4*–*6*, *8*–*10*, *12*, *16*–*21*).

We report a room-temperature photochemical strategy to fabricate a highly stable, atomically dispersed Pd catalyst (Pd_1/TiO_2) on ultrathin TiO_2 nanosheets with Pd loading up to 1.5%.

[1]State Key Laboratory for Physical Chemistry of Solid Surfaces, Collaborative Innovation Center of Chemistry for Energy Materials, Engineering Research Center for Nano-Preparation Technology of Fujian Province, National Engineering Laboratory for Green Chemical Productions of Alcohols, Ethers, and Esters, and Department of Chemistry, College of Chemistry and Chemical Engineering, Xiamen University, Xiamen 361005, China. [2]Institute of Physics, Chinese Academy of Sciences, Beijing 100190, China. [3]Department of Chemistry, Dalhousie University, Halifax, Nova Scotia B3H 4R2, Canada.
***Corresponding author. Email: nfzheng@xmu.edu.cn (N.Z.);**

Large optical nonlinearity of indium tin oxide in its epsilon-near-zero region

M. Zahirul Alam, Israel De Leon, and Robert W. Boyd

Science **352** (6287), . DOI: 10.1126/science.aae0330

Nonlinear optics: A surprise in store?

At ultrafast data rates, the ability to use light to control things could speed information processing. However, photons tend not to interact with each other, and so a nonlinear optical material is needed and the response of such materials is typically weak. Alam *et al.* report a surprising finding: that indium tin oxide, a commercially available transparent conducting oxide widely used in microelectronics, exhibits a large nonlinear response. They used a wavelength regime where the permittivity of the material is close to zero and observed a large and fast nonlinear optical response. The finding offers the possibility that other, so far unexplored, materials may be out there for nonlinear optical applications.

Science, this issue p. 795